[redacted]

Copy 4

RM A57F06b

NACA RM A57F06b

C/

NACA

RESEARCH MEMORANDUM

EFFECTS OF WING-TIP DROOP ON THE LONGITUDINAL CHARACTERISTICS OF TWO HIGHLY SWEPT WING-BODY COMBINATIONS AT MACH NUMBERS FROM 0.6 TO 1.4

By Earl D. Knechtel and George Lee

Ames Aeronautical Laboratory
Moffett Field, Calif.

CLASSIFICATION CHANGED
UNCLASSIFIED

To

By authority of Nasa TPA9 Effective Date 7-22-59
NB 12-54-59

NATIONAL ADVISORY COMMITTEE FOR AERONAUTICS

WASHINGTON

August 30, 1957

[redacted]

UNCLASSIFIED

NATIONAL ADVISORY COMMITTEE FOR AERONAUTICS

RESEARCH MEMORANDUM

EFFECTS OF WING-TIP DROOP ON THE LONGITUDINAL CHARACTERISTICS OF TWO HIGHLY SWEPT WING-BODY COMBINATIONS AT MACH NUMBERS FROM 0.6 TO 1.4

By Earl D. Knechtel and George Lee

SUMMARY

An investigation was conducted to determine the effects of wing-tip droop on the longitudinal stability characteristics of a 53° and a 63° sweptback wing-body combination. Both models were tested with flat and abruptly drooped wing tips. The 63° wing was also tested with a curved drooped tip. In addition, the combined effects of wing fences and extended leading-edge flaps were investigated. The results showed that abrupt droop of the outer 40 percent of the basic 53° wing improved the stability characteristics of the model. For the 63° swept wing, curved droop caused slight beneficial effects on the stability, whereas abrupt droop caused adverse effects. In general, the most favorable stability characteristics were obtained for either flat or abruptly drooped wings with fences and extended leading-edge flaps.

INTRODUCTION

The longitudinal instability of swept wings at subsonic and transonic speeds at moderate to high angles of attack has been the subject of numerous investigations in recent years (refs. 1 to 6). The instability has been traced to flow separation which initially begins at the outboard portion of the wing. The flow separation is due to (1) the outboard portion being more highly loaded than the inboard portion, and (2) the maximum lift of the outboard portion being only slightly affected by spanwise boundary-layer flow, whereas maximum lift of the inboard portion is greatly increased by spanwise flow. Various devices have been employed to alleviate flow separation near the wing tips. One type of such devices is intended to increase the maximum lift of sections near the tips, and includes increased leading-edge radius, leading-edge slats or flaps, and camber. Another type of modification is intended to reduce the loading of sections near the tips, an example being wing twist. The third, and perhaps more successful, type of modification is intended to control or alter the spanwise flow on the wing. The latter group would include boundary-layer fences and leading-edge chord extensions on the outer portion of the wing.

A modification which might be classified as having the combined effects of two of the above types involves the use of extreme amounts of negative dihedral over the tip portion of the swept wing. Possible advantages of drooped tips are, first, that the angle of attack would increase more slowly at the tip than at the inboard part of the wing, and, second, that the discontinuity of the droop might favorably alter the spanwise boundary-layer flow. Blackaby (ref. 7) has shown that at low speeds abrupt droop of the tip produced improvements in the stability characteristics of a 63° swept wing comparable to those caused by addition of a wing fence. The present investigation was conducted to determine, for wing-body combinations having 53° and 63° of sweep, the effects of wing-tip droop on the longitudinal stability characteristics at transonic speeds, both alone and in combination with fences and extended leading-edge flaps on the outboard portion of the wing.

NOTATION

c	local wing chord
$\bar{c}$	mean aerodynamic chord
C_D	drag coefficient, $\frac{\text{drag}}{qS}$
$C_{D_{min}}$	minimum drag coefficient
C_L	lift coefficient, $\frac{\text{lift}}{qS}$
$C_{L_{opt}}$	lift coefficient for $\left(\frac{L}{D}\right)_{max}$
C_{L_α}	lift-curve slope
C_m	pitching-moment coefficient about an axis through the quarter-chord points of the mean aerodynamic chords, $\frac{\text{pitching moment}}{qS\bar{c}}$
$\frac{dC_m}{dC_L}$	pitching-moment-curve slope
$\Delta\frac{dC_m}{dC_L}$	change in pitching-moment-curve slope from that at zero lift

$\frac{L}{D}$	lift-drag ratio
$\left(\frac{L}{D}\right)_{max}$	maximum lift-drag ratio
M	free-stream Mach number
q	free-stream dynamic pressure
r	body radius
S	total plan-form area of basic wing
x	axial coordinate, measured from body nose
α	angle of attack, deg
Λ	leading-edge sweep, deg

APPARATUS AND MODELS

The investigation was conducted in the Ames 2- by 2-foot transonic wind tunnel. The test section of this wind tunnel is ventilated, allowing continuous choke-free operation through the range of Mach numbers up to 1.4. This facility is described in detail in reference 8.

The models were constructed of steel and all were derived from, or were direct modifications of, two basic wing plan forms. The first basic configuration (fig. 1(a)), one of those for which longitudinal characteristics were presented in reference 6, had 53° sweep of the leading edge, an aspect ratio of 3.0, a taper ratio of 0.4, and NACA 0003 airfoil sections in the streamwise direction. The second basic plan form was that employed in references 1 to 3, having 63° sweep of the leading edge, an aspect ratio of 3.5, and a taper ratio of 0.25. As shown in figure 1(b), the 63° swept wing in the present case had a 6-percent-thick modified-flat-plate airfoil section (streamwise) with rounded leading edge and wedge-shaped trailing edge. The wings in each case were attached to a modified Sears-Haack body of 9.85 fineness ratio.

From the two basic models, a total of four wing-body configurations for the 53° swept wing and five for the 63° swept wing were derived. The first four configurations were similar for both models. These are (1) the basic wing, (2) the wing with a fence and extended leading-edge flap on the outboard portion of the wing, (3) the wing with tips abruptly drooped 40° outboard of 0.6 semispan, and (4) the wing with drooped tips as well as the auxiliary lift devices of (2). The fifth configuration for the

63° wing consisted of the wing with the portion outboard of 0.4 semispan curved downward at constant radius to 45° slope at the tip.

It is to be noted that of the four models with auxiliary lift devices (configurations (2) and (4)), three had the fence and the inboard end of the leading-edge flap located at 0.6 semispan. However, on the flat 53° wing with auxiliary devices, the fence and flap were inadvertently located somewhat farther inboard (at 0.48 semispan) as shown in figure 1(a).

The models were sting-supported in the test section, as shown in figure 2. Forces and moments were measured by an internal strain-gage balance. The area blockage ratios of the basic models at zero angle of attack were approximately 0.005 for the 53° wing and 0.006 for the 63° wing.

TESTS AND DATA REDUCTION

Lift, drag, and pitching moment were measured at angles of attack from -4° to 22° at Mach numbers from 0.6 to 1.4. A Reynolds number of 1.5 million based on the mean aerodynamic chord was held constant for angles of attack up to the load limit of the balance, or approximately 12°. For higher angles of attack, the tunnel stagnation pressure, and hence the Reynolds number, was reduced by as much as 30 percent because of balance load limits. All coefficients are based on the basic wing plan-form geometry.

Model base pressures were recorded and used to adjust the measured drag to correspond to a condition of free-stream static pressure at the model base. Angles of attack were corrected for deflections of the sting and balance resulting from aerodynamic loads.

Subsonic wall interference effects as shown in reference 8 were small enough to require no corrections for models of the size employed in the present investigation. Interference caused by wall-reflected shock waves at Mach numbers from 1.06 to 1.15 are known to be present; however, no assessment of their effects has been made. No attempt has been made to correct the data for the effects of aeroelastic distortion.

Apart from possible systematic errors resulting from neglecting the above corrections, the probable random errors in the data near zero lift, as determined by a root-mean-square analysis of data scatter, are considered to be as follows:

M ±0.003
α ±0.03°
C_L ±0.008
C_m ±0.006
C_D ±0.0010

RESULTS AND DISCUSSION

Lift, drag, and pitching-moment results for the models are presented in figures 3, 4, and 5, respectively. The variation of lift-curve slope with Mach number at three lift coefficients is presented in figure 6. Figures 7, 8, and 9, respectively, show the variations with Mach number of minimum drag coefficient, maximum lift-drag ratio, and lift coefficient for maximum lift-drag ratio ($C_{L_{opt}}$). The variation of pitching-moment-curve slope with Mach number at constant lift coefficient is plotted in figure 10. Presented in figure 11 are the variations with Mach number of the lift coefficient for a given reduction in longitudinal stability from that at zero lift, as measured by a value of $\Delta(dC_m/dC_L)$ of 0.12.

Lift

The model with 53° of sweep.- The effect of abrupt wing-tip droop on the lift-curve slope (fig. 6) was generally small throughout the Mach number range of the tests. The two configurations with drooped tips had slightly lower lift-curve slopes than the corresponding models without droop. The addition of fences and leading-edge flaps to the basic 53° swept wing increased the lift-curve slope by amounts ranging up to 20 percent at zero lift.

The range of angle of attack was insufficient for defining the effect of the modifications on maximum lift. The lift curves (fig. 3) show, however, that at the highest angles of attack, the lift coefficients of the flat wing with fence and leading-edge flap were generally higher than those of the other four configurations.

The model with 63° of sweep.- The variation of lift with angle of attack for the 63° models indicated trends similar to those previously discussed for the 53° models. The configurations having curved or abruptly drooped tips usually had the lowest lift-curve slopes. The flat wing with fences and leading-edge flaps had the highest lift-curve slopes as well as the highest lift coefficient at the larger angles of attack.

Drag

The model with 53° of sweep.- Examination of the drag results shows that drooping the tips of the basic wing caused little change in the minimum drag coefficient (fig. 7(a)) and decreased the maximum lift-drag ratio (fig. 8(a)). The addition of fences and leading-edge flaps to the flat wing and to the abruptly drooped wing caused a substantial increase in the minimum drag coefficient as expected, and also reduced the maximum lift-drag ratio. The maximum lift-drag ratios were highest for the basic flat wing and lowest for the drooped wing with fences and flaps. However, as indicated by the drag polars (fig. 4), the addition of fences and leading-edge flaps improved the drag characteristics at moderate to high lift. This effect is also indicated in figure 9(a), where the optimum lift coefficient is seen to have been increased by the addition of these auxiliary devices. Addition of wing-tip droop to the basic wing caused the optimum lift coefficient to decrease slightly for Mach numbers up to 1.1 and increase slightly for higher Mach numbers.

The model with 63° of sweep.- The unfavorable drag characteristics of the modified flat-plate wing are reflected in its higher values of $C_{D_{min}}$ and lower values of $(L/D)_{max}$ than those shown for this plan form with more conventional wing sections in reference 1. As in the case of the 53° swept wings, the addition of fences and leading-edge flaps to the flat wing and to the abruptly drooped wing caused significant increases in both minimum drag coefficient and optimum lift coefficient. Other effects of these devices were slight increases in maximum lift-drag ratio for the flat wing and slight decreases for the abruptly drooped wing.

Abrupt droop of the basic wing caused slight increases in minimum drag and little or no change in either maximum lift-drag ratio or optimum lift coefficient. Curved droop caused small increases in minimum drag and small decreases in maximum lift-drag ratio, as well as slight decreases in optimum lift coefficient at subsonic speeds and slight increases at supersonic speeds.

Pitching Moment

The pitch-up of swept-wing airplanes is basically a dynamic phenomenon. Therefore, an accurate definition of potentially dangerous pitch-up conditions requires a dynamic stability analysis to take into account other factors in addition to the static pitching-moment characteristics. For the purpose of this report, a dynamic stability analysis was not considered warranted; however, it was considered desirable to provide some basis of comparison of the pitch-up tendencies of the various configurations. For this purpose it was convenient to define the lift coefficient for pitch-up tendency as the lift coefficient for which the pitching-moment-curve slope had increased by approximately 0.12 from the slope at zero lift. This definition is approximately analogous to comparing the stability boundaries of the various configurations based on the usual stability criterion, $dC_m/dC_L = 0$, after adjusting all the pitching-moment curves to have a common slope, $dC_m/dC_L = -0.12$, at zero lift.

The model with 53° of sweep.- Abrupt drooping of the wing tips increased the lift coefficient for pitch-up tendency substantially throughout most of the Mach number range (fig. 11(a)). Increases in stability-boundary lift coefficients of 0.1 to 0.25 over those of the basic wing were obtained at subsonic speeds up to $M = 0.95$. Small improvements were again obtained for Mach numbers greater than 1.05 and these gains increased with Mach number. Addition of fences and leading-edge flaps caused the stability at moderate lifts to increase for Mach numbers up to 0.96 (see fig. 5(a)). The greatest improvement in stability over the complete Mach number range was obtained for the model having drooped wing tips together with fences and leading-edge flaps. For this configuration, stability-boundary lift coefficients 0.35 higher than for the basic wing were obtained at subsonic speeds, while at Mach numbers from 1.02 to 1.30 no unstable tendencies were noticed for angles of attack up to 22°. Addition of fences and extended leading-edge flaps to the basic wing increased the stability-boundary lift coefficients by approximately 0.4 at Mach numbers up to 0.92 and by 0.10 to 0.25 at Mach numbers above 1.03. The decreased effectiveness of the fences and extended leading-edge flaps at high subsonic speeds was attributed to their inability to control flow separation on the wing caused by the strong shock waves associated with deceleration of the entire three-dimensional flow field.

Drooping the wing tips decreased the stability at zero lift (fig. 5(a)). This effect is further illustrated in the lower part of figure 10(a), where tip droop is shown to increase dC_m/dC_L by amounts ranging from 0.07 at subsonic speeds to about 0.03 at a Mach number of 1.4.

<u>The model with 63° of sweep</u>.- Figure 11(b) indicates that neither the curved nor abrupt droop eliminated the pitch-up tendency, although curved droop caused slight to moderate improvements over the basic wing up to Mach number of 1.1. Throughout most of the range of Mach numbers, the change to abruptly drooped wing tips reduced the stability-boundary lift coefficients by 0.1 to 0.2. This effect of abrupt droop contrasts with that reported in reference 7, which indicated that, at low speeds, abrupt droop improved the longitudinal stability of a wing-body combination having this same plan form. It should be noted, however, that the sections of the two wings were different, the wing of the present investigation having a modified flat-plate airfoil with a large leading-edge radius rather than a conventional airfoil section such as those employed in the reference investigations. The effect of this difference in wing section on the pitching-moment characteristics can be illustrated by comparing the data of the present investigation with those of reference 1 at comparable Mach numbers. This comparison shows that the wing with a conventional section (NACA 64A006) had a much more severe pitch-up tendency.

The addition of fences and extended leading-edge flaps, either with or without abrupt droop, increased the lift coefficient for pitch-up tendency by 0.1 over that of the basic wing for Mach numbers up to 0.9, and generally produced the most satisfactory pitching-moment characteristics.

CONCLUSIONS

The results of an experimental investigation of the effects of wing-tip droop on the longitudinal aerodynamic characteristics of highly swept wings with and without fences and extended leading-edge flaps at Mach numbers from 0.6 to 1.4 lead to the following conclusions:

1. For 53° of sweep

(a) Abrupt drooping of the outboard 40 percent of the basic wing improved the pitching-moment characteristics substantially.

(b) The most favorable pitching-moment characteristics were obtained for the flat wing with fences and leading-edge flaps at Mach numbers up to 0.9, and for the abruptly drooped wing with fences and leading-edge flaps for Mach numbers greater than 0.9.

(c) Addition of fences and leading-edge flaps caused the maximum lift-drag ratios to be lower, and the lift coefficient for maximum lift-drag ratio to be higher, than those of the configurations without the auxiliary devices.

2. For 63° of sweep

(a) Abrupt drooping of the outboard 40 percent of the basic wing caused an adverse effect on the pitching-moment characteristics, while curved droop had a slight beneficial effect.

(b) In general, the most favorable pitching-moment characteristics were obtained for either the flat or abruptly drooped wing with fences and leading-edge flaps.

(c) The flat wing with fences and leading-edge flaps had the highest maximum lift-drag ratios.

Ames Aeronautical Laboratory
National Advisory Committee for Aeronautics
Moffett Field, Calif., June 6, 1957

REFERENCES

1. Reynolds, Robert M., and Smith, Donald W.: Aerodynamic Study of a Wing-Fuselage Combination Employing a Wing Swept Back 63°. - Subsonic Mach and Reynolds Number Effects on the Characteristics of the Wing and on the Effectiveness of an Elevon. NACA RM A8D20, 1948.

2. Mas, Newton A.: Aerodynamic Study of a Wing-Fuselage Combination Employing a Wing Swept Back 63°. - Characteristics for Symmetrical Wing Sections at High Subsonic and Moderate Supersonic Mach Numbers. NACA RM A9E09, 1949.

3. Madden, Robert F.: Aerodynamic Study of a Wing-Fuselage Combination Employing a Wing Swept Back 63°. - Characteristics at a Mach Number of 1.53 Including Effect of Small Variations of Sweep. NACA RM A8J04, 1949.

4. Weiberg, James A., and Carel, Hubert C.: Wind-Tunnel Investigation at Low Speed of a Wing Swept Back 63° and Twisted and Cambered for a Uniform Load at a Lift Coefficient of 0.5. NACA RM A50A23, 1950.

5. Madden, Robert T.: Aerodynamic Study of a Wing-Fuselage Combination Employing a Wing Swept Back 63°. - Investigation at a Mach Number of 1.53 to Determine the Effects of Cambering and Twisting the Wing for Uniform Load at a Lift Coefficient of 0.25. NACA RM A9C07, 1949.

6. Knechtel, Earl D., and Summers, James L.: Effects of Sweep and Taper Ratio on the Longitudinal Characteristics of an Aspect Ratio 3 Wing-Body Combination at Mach Numbers From 0.6 to 1.4. NACA RM A55A03, 1955.

7. Blackaby, James R.: Wind-Tunnel Investigation at Low Speed of a Wing Having 63° Sweepback and a Drooped Tip. NACA RM A55B14, 1955.

8. Spiegel, Joseph M., and Lawrence, Leslie F.: A Description of the Ames 2- by 2-Foot Transonic Wind Tunnel and Preliminary Evaluation of Wall Interference. NACA RM A55I21, 1956.

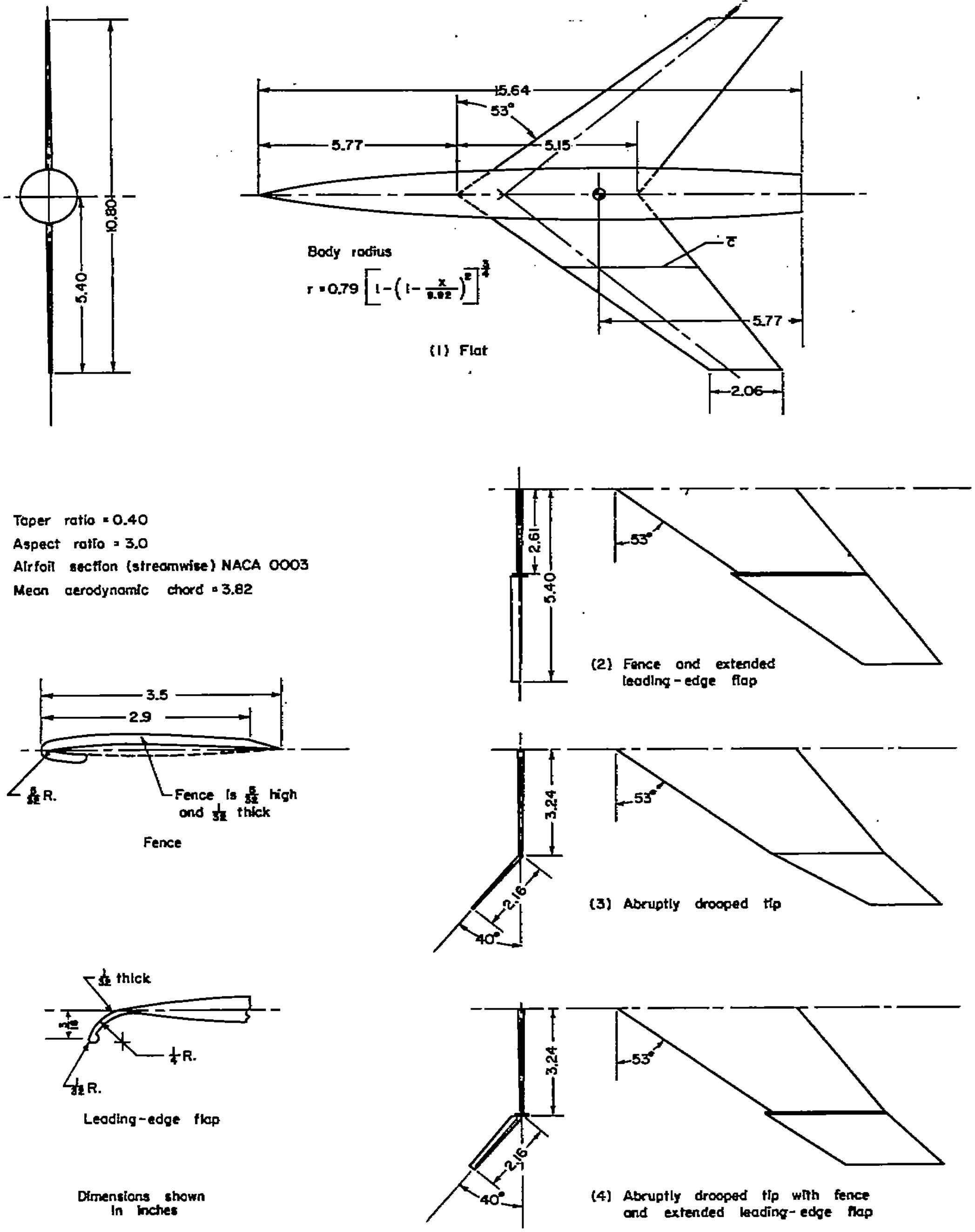

(a) $\Lambda = 53°$

Figure 1.- Geometric details of basic models and modifications.

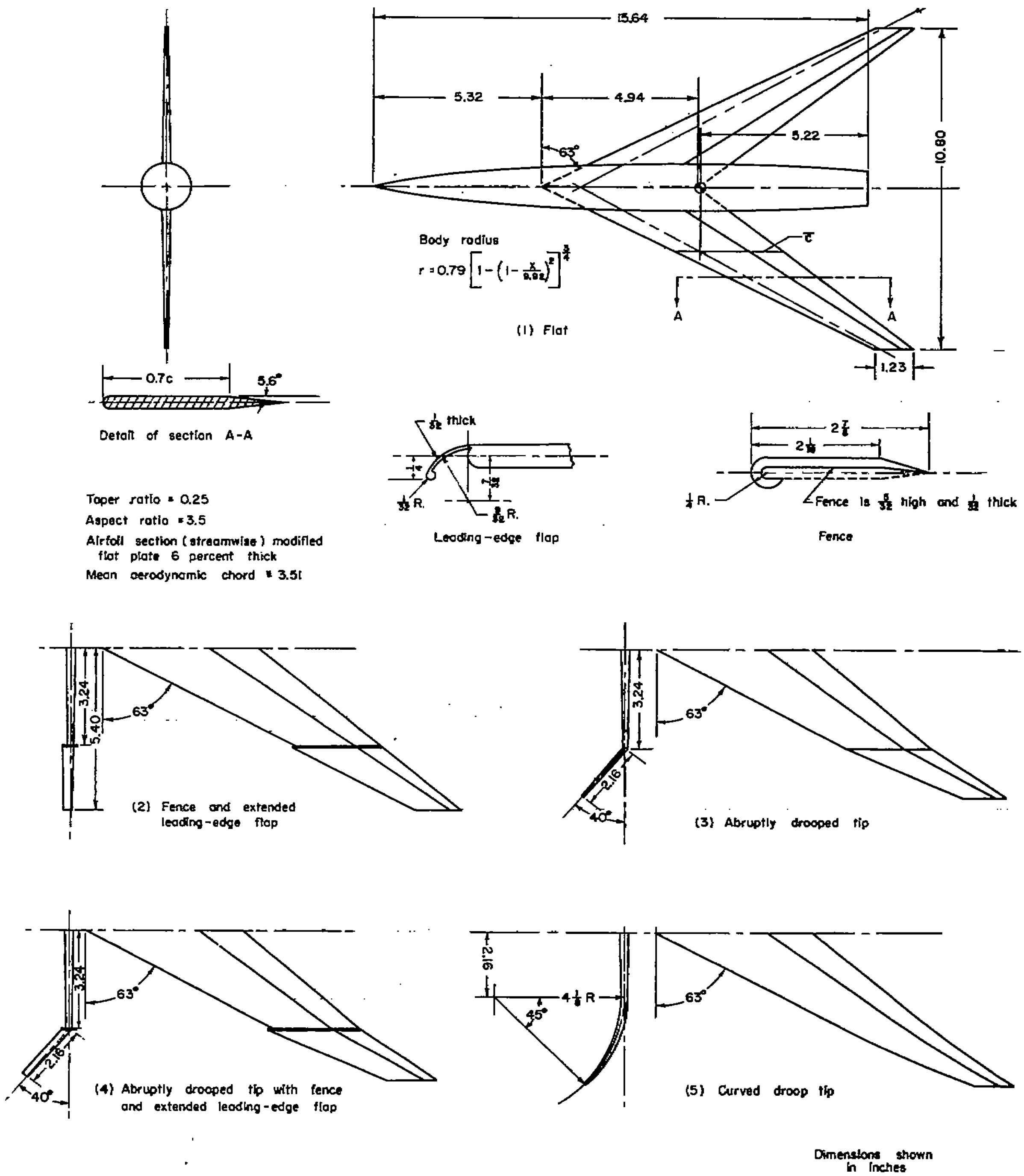

(b) Λ = 63°

Figure 1.- Concluded.

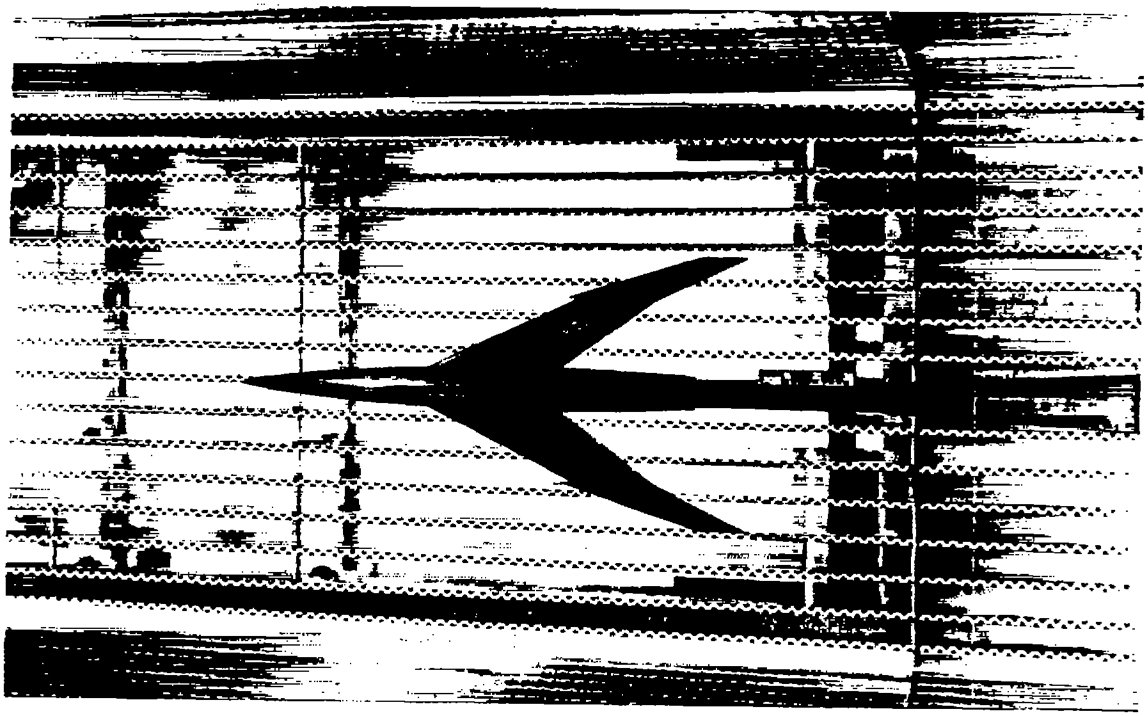

A-20249

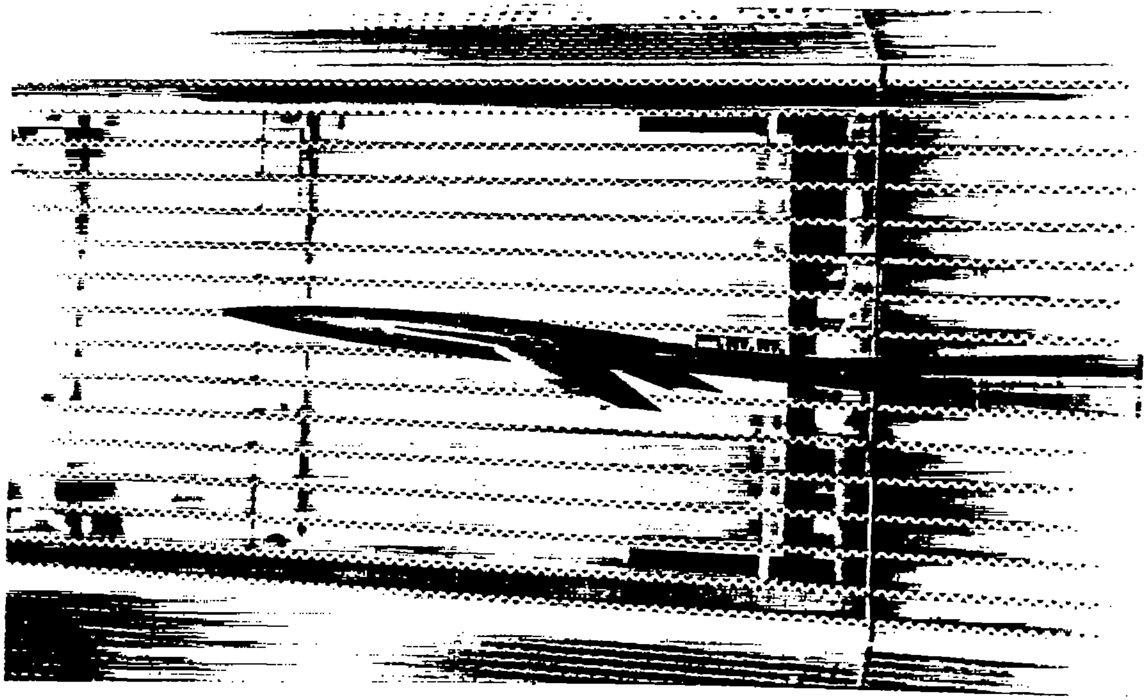

A-20250

Figure 2.- Two views of model installed in the Ames 2-by 2-foot transonic wind tunnel.

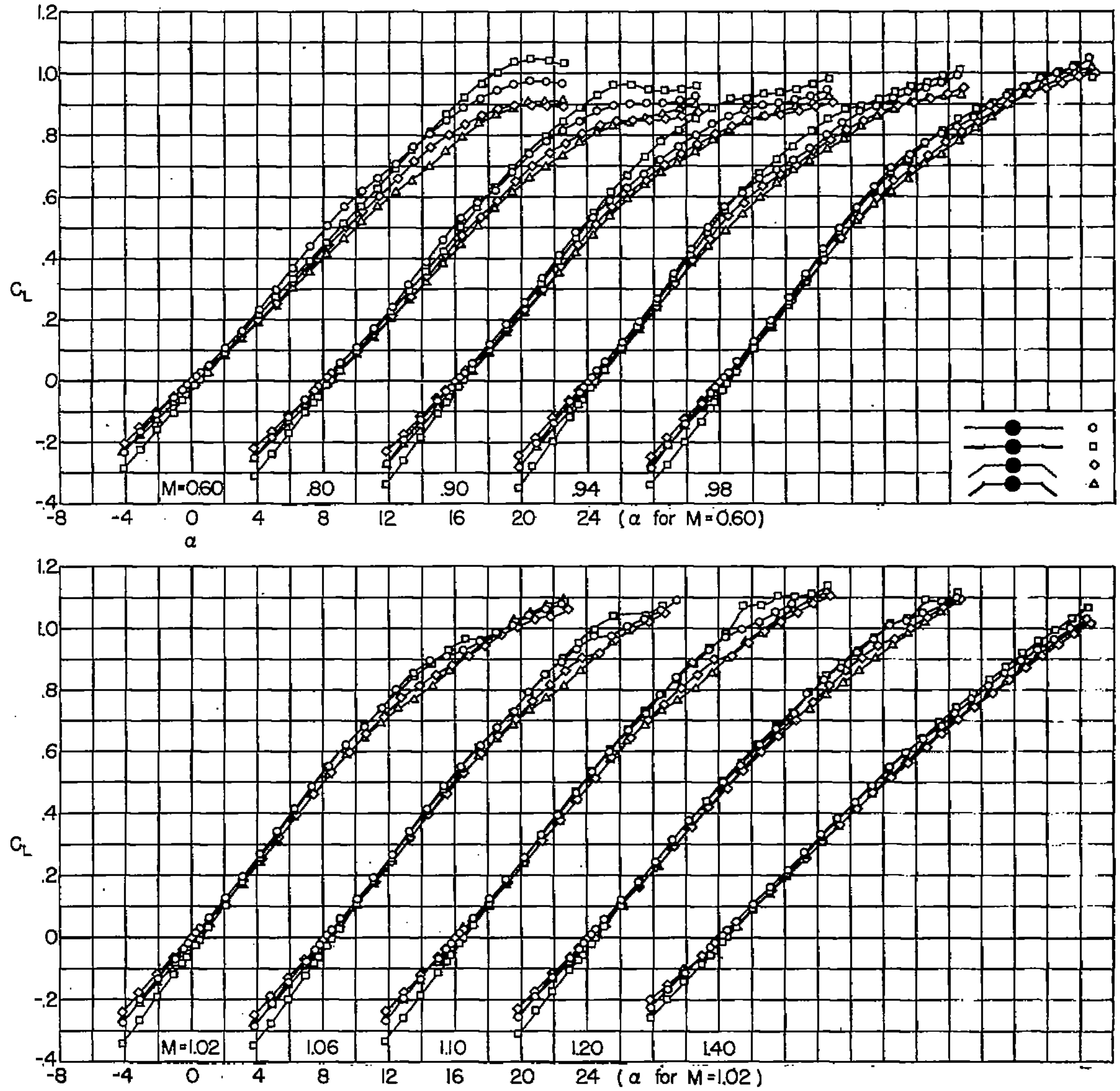

(a) Λ = 53°

Figure 3.- Variation of lift coefficient with angle of attack at constant Mach number.

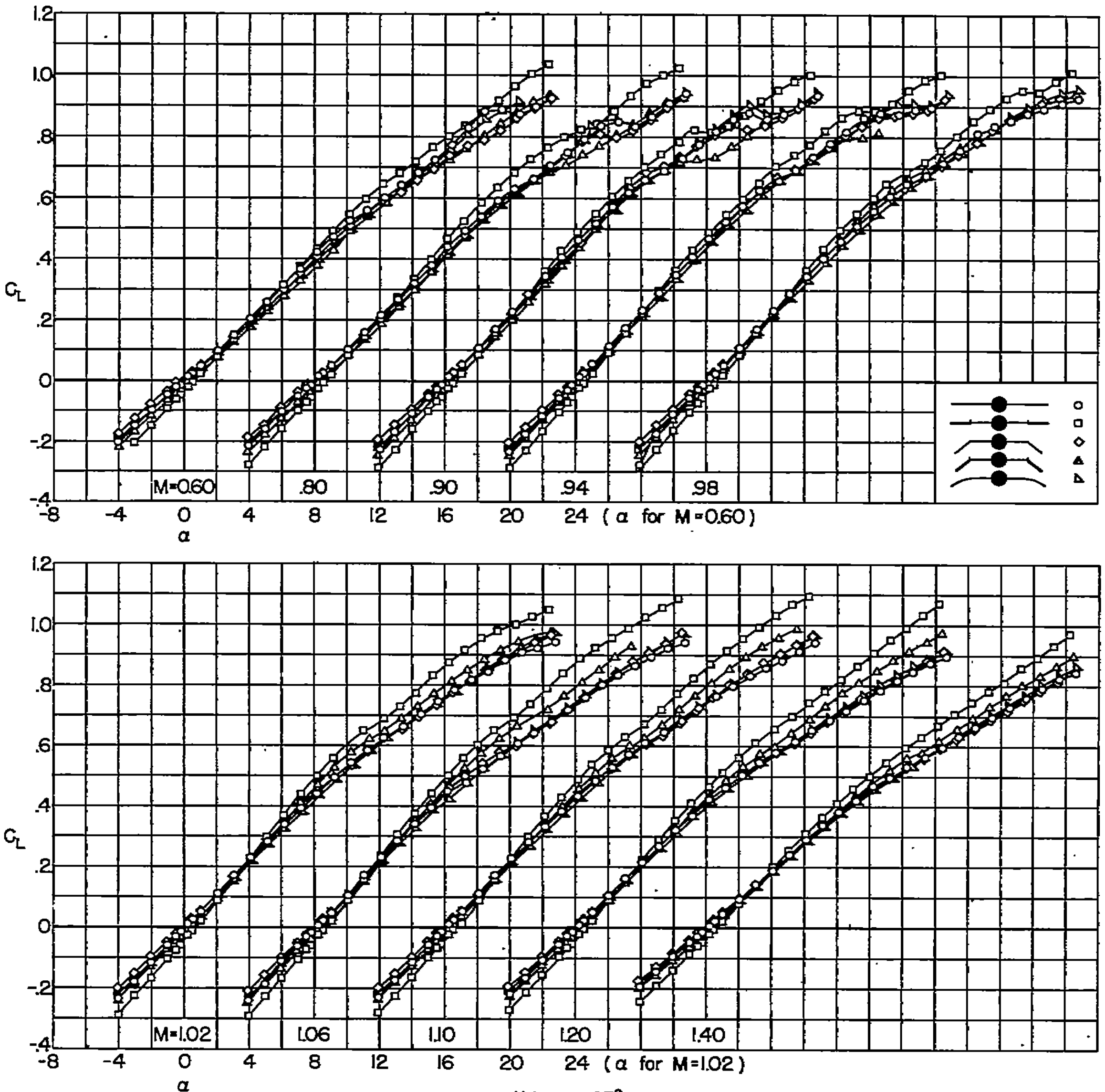

(b) Λ = 63°

Figure 3.- Concluded.

[redacted]

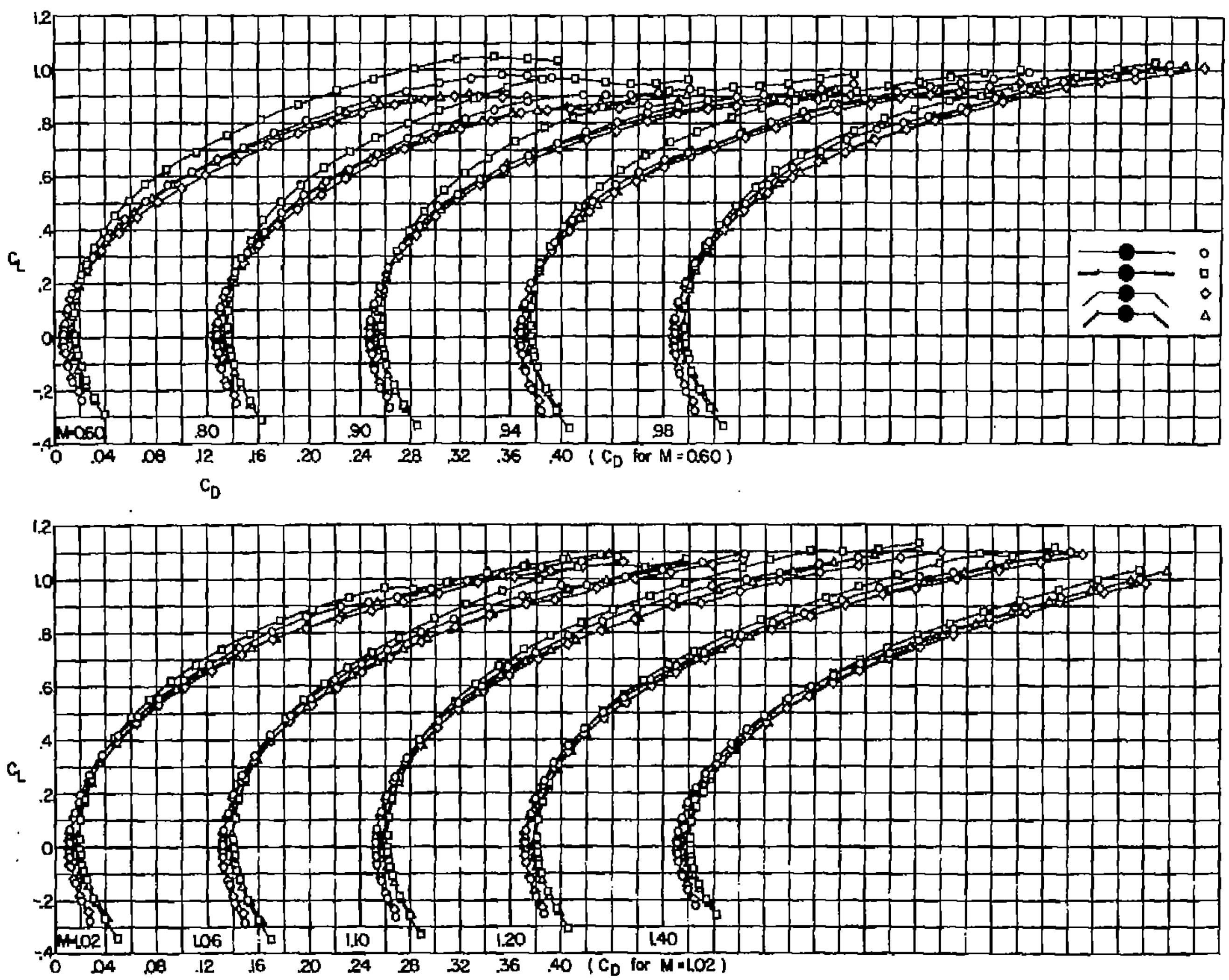

(a) $\Lambda = 53°$

Figure 4.- Variation of drag coefficient with lift coefficient at constant Mach number.

[redacted]

[redacted]

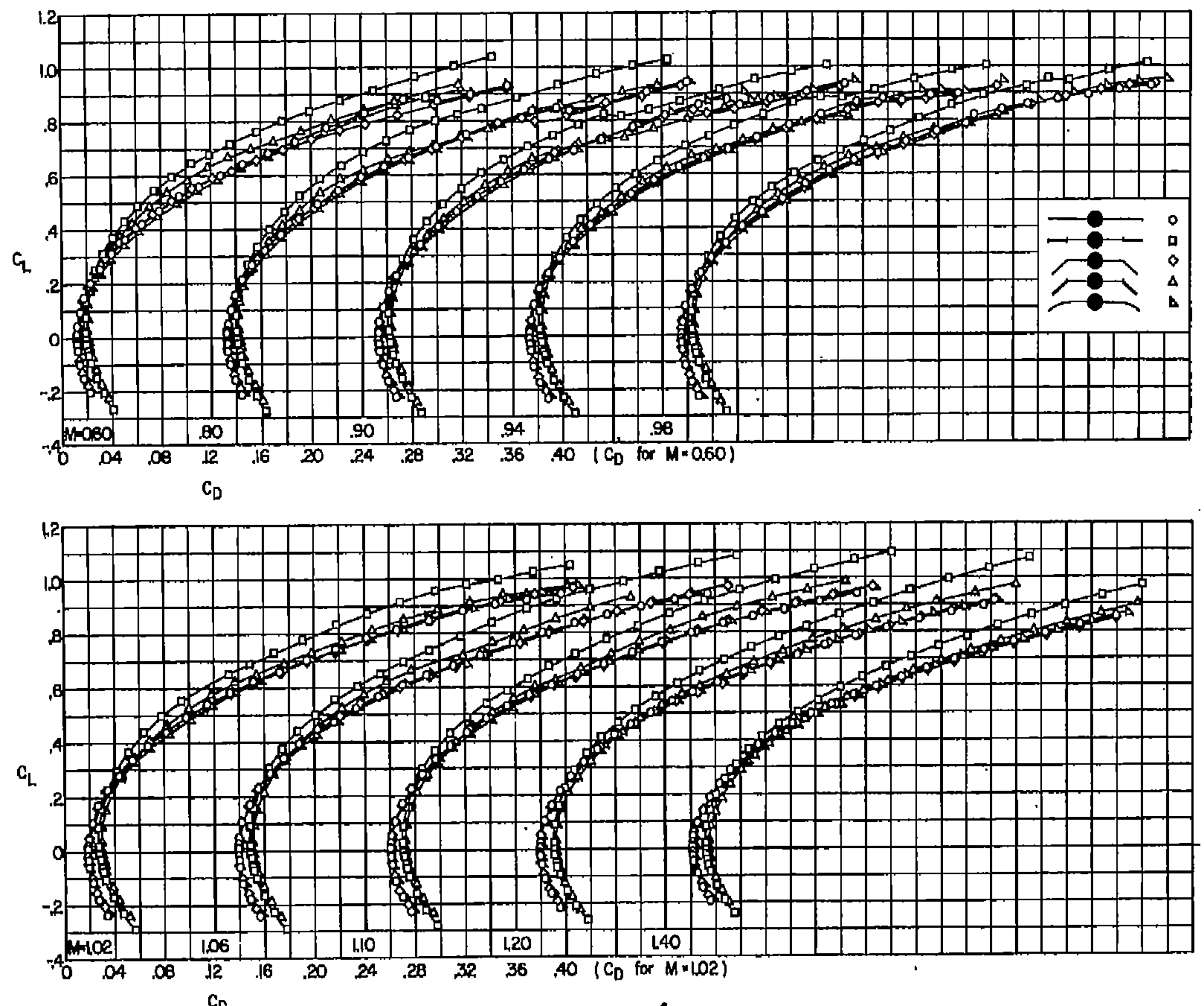

(b) $\Lambda = 63°$

Figure 4.- Concluded.

3Q

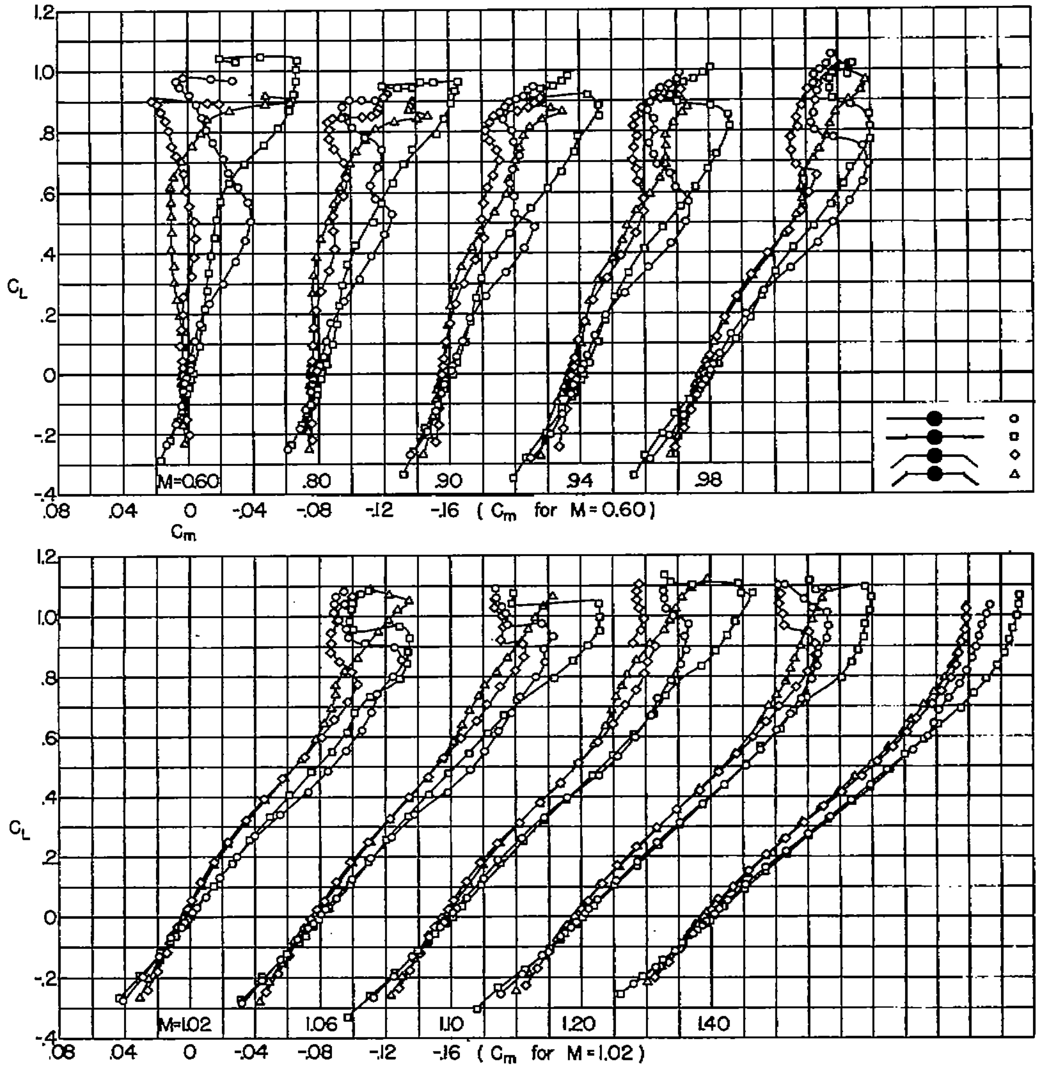

(a) Λ = 53°

Figure 5.- Variation of pitching-moment coefficient with lift coefficient at constant Mach number.

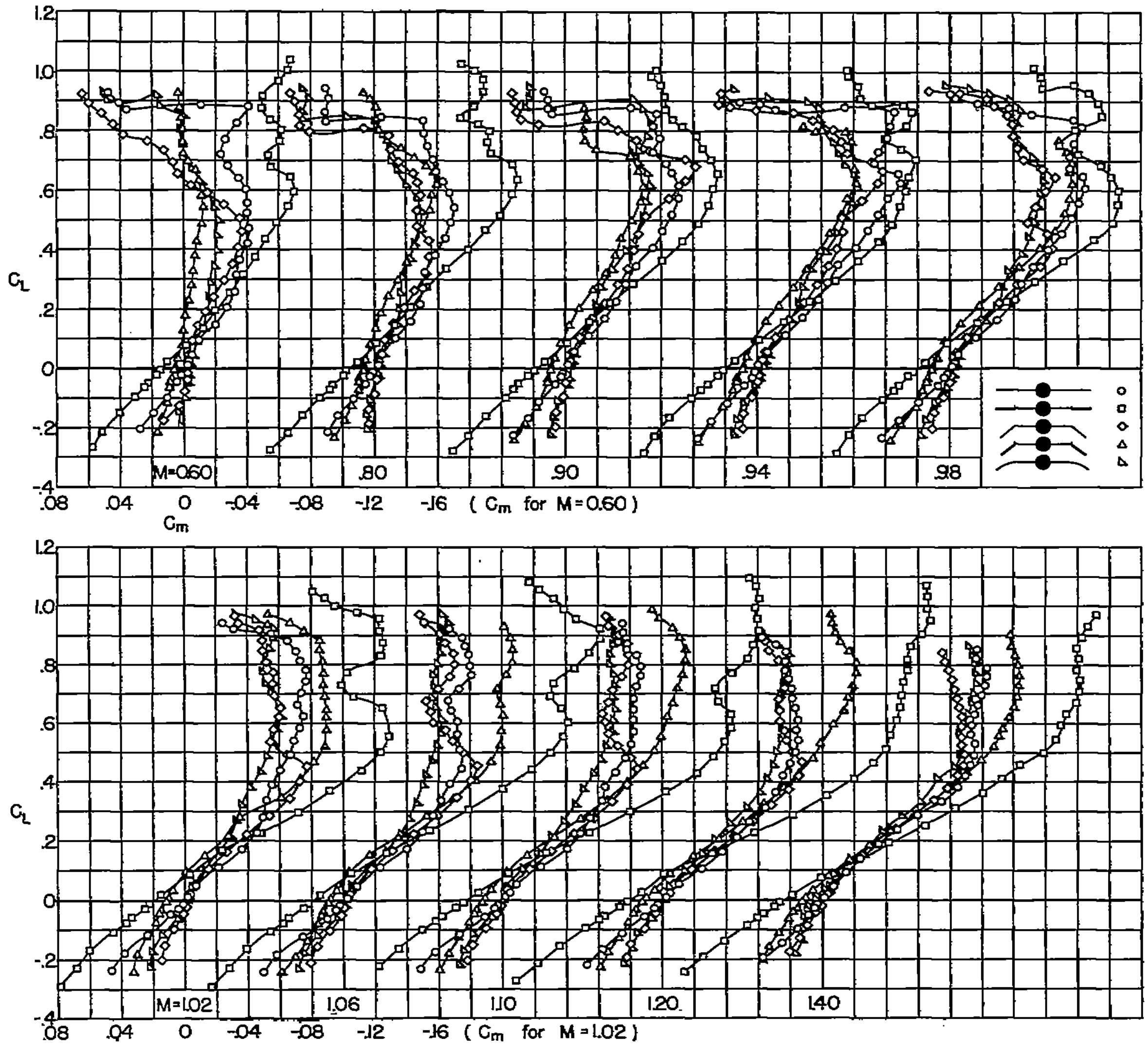

(b) Λ = 63°

Figure 5.- Concluded.

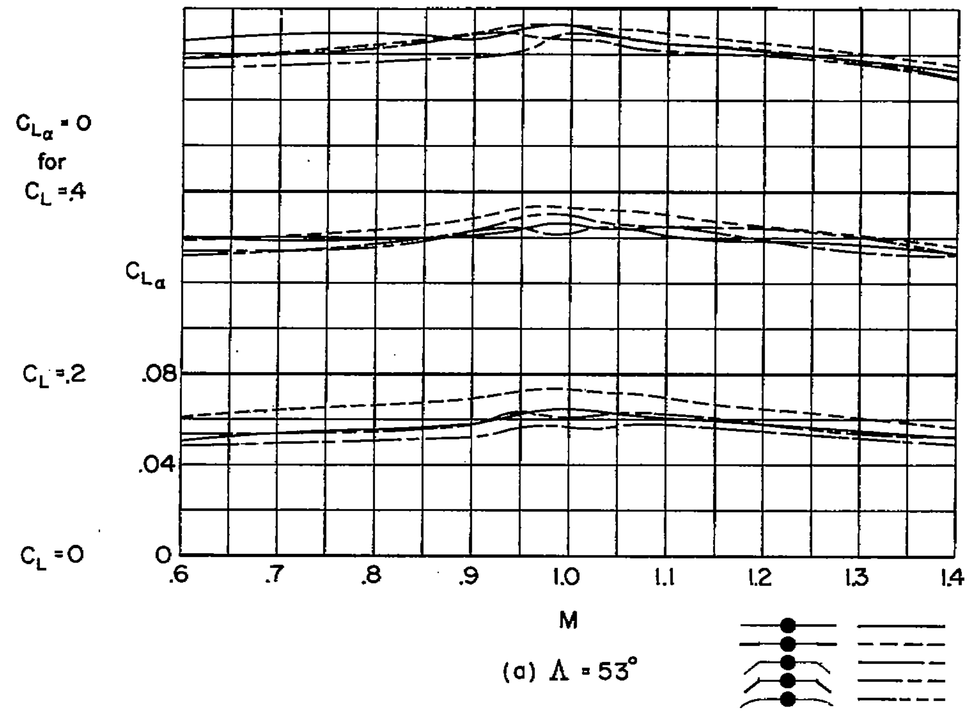

(a) $\Lambda = 53°$

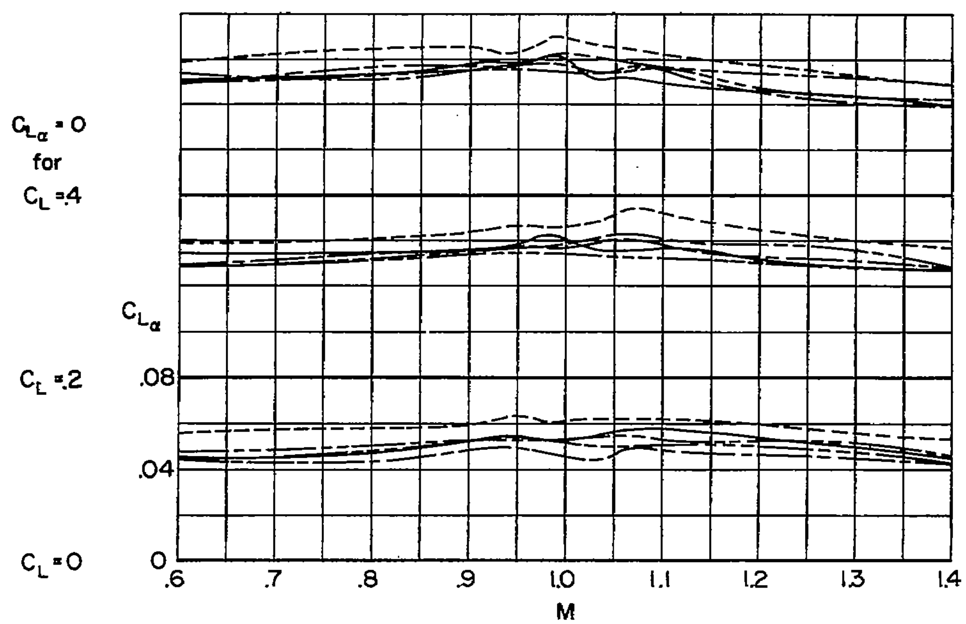

(b) $\Lambda = 63°$

Figure 6.- Variation of lift-curve slope with Mach number at constant lift coefficient.

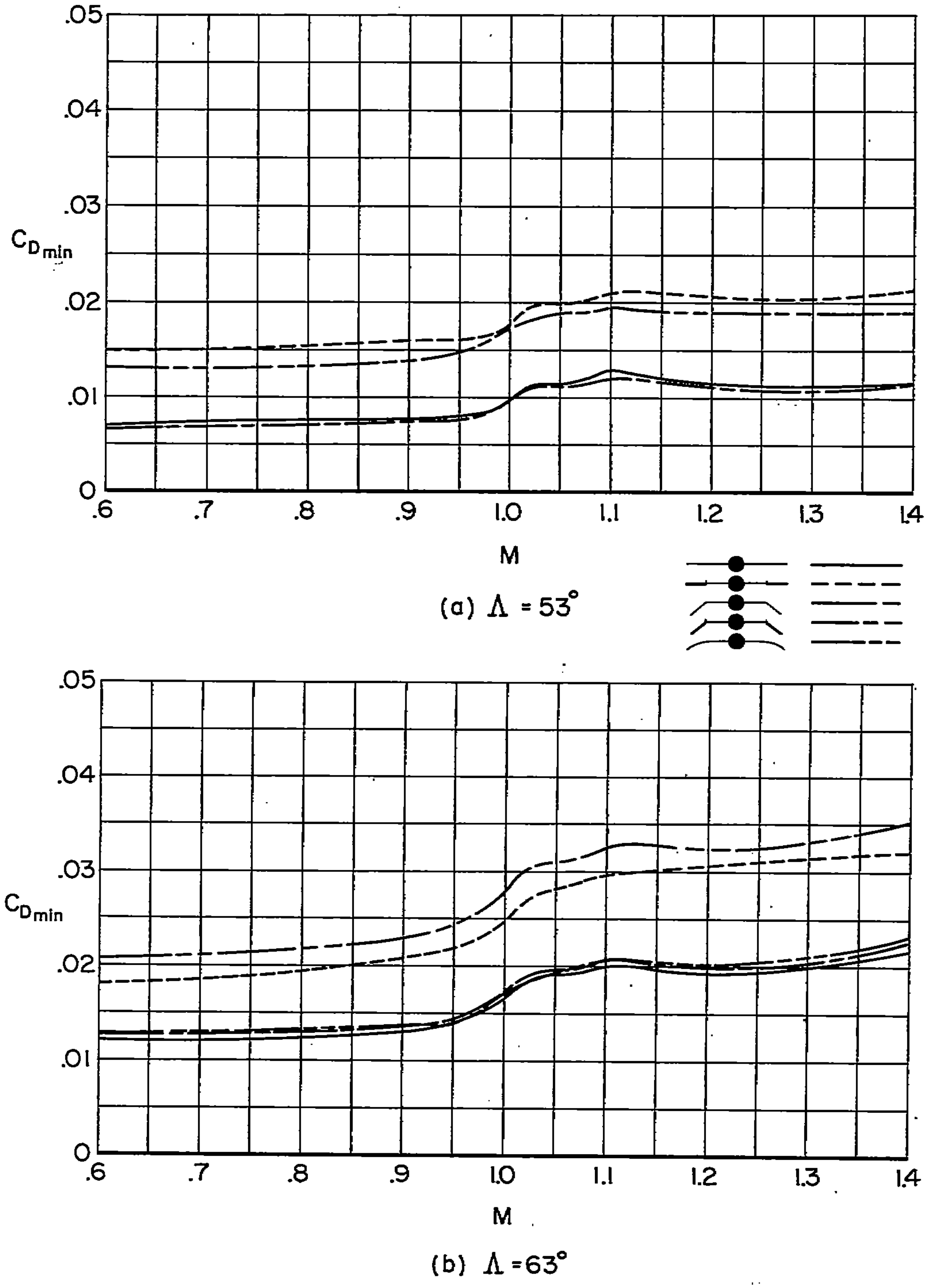

Figure 7.- Variation of minimum drag coefficient with Mach number.

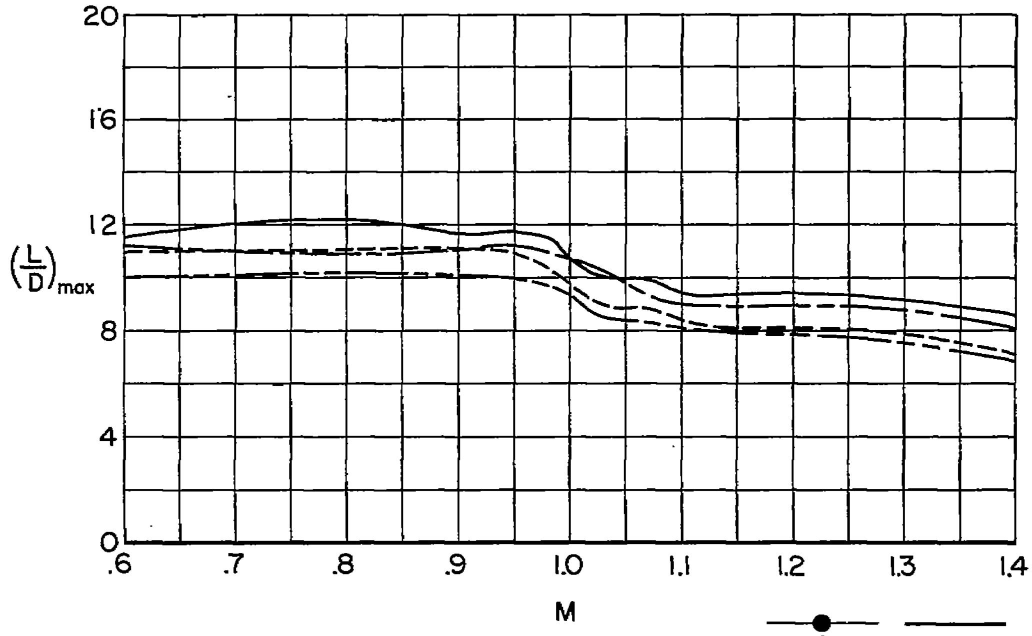

(a) $\Lambda = 53°$

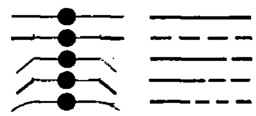

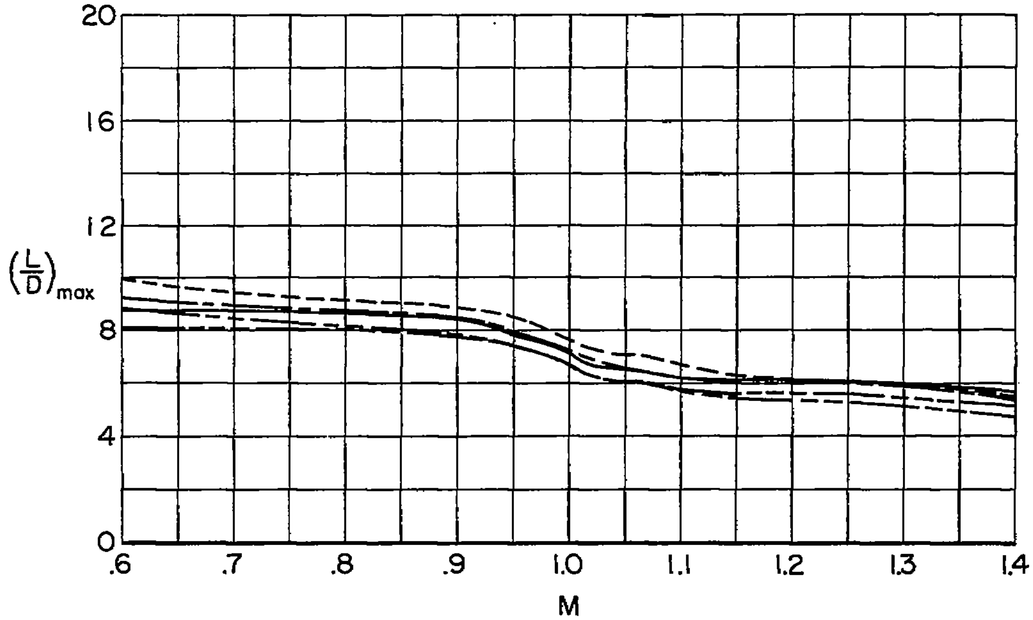

(b) $\Lambda = 63°$

Figure 8.- Variation of maximum lift-drag ratio with Mach number.

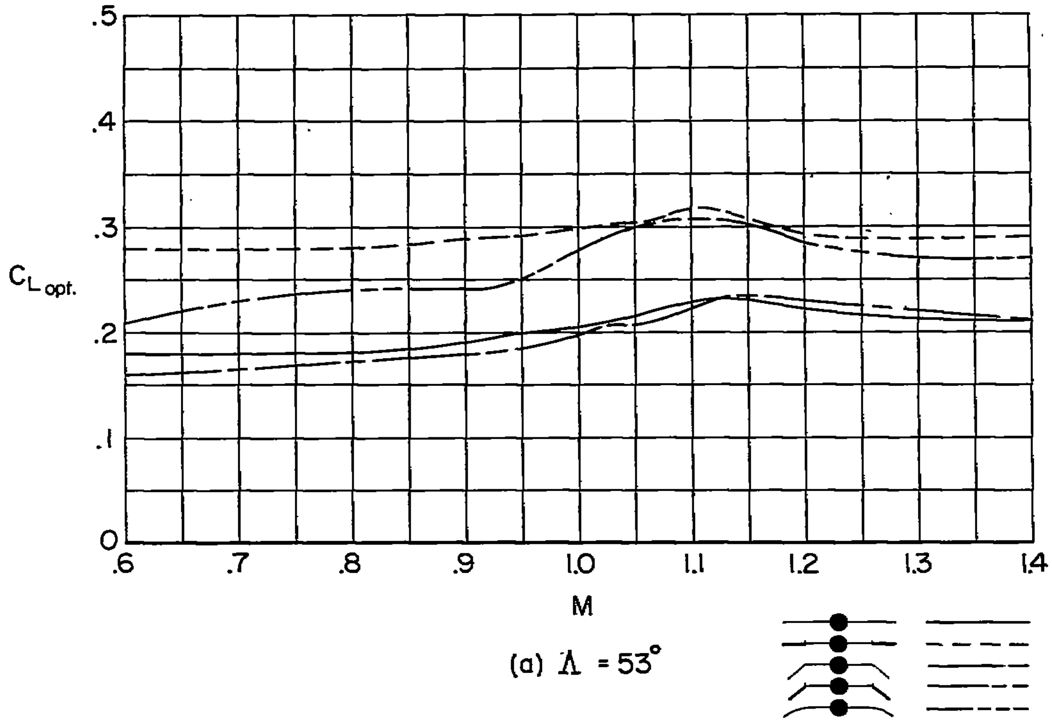

(a) $\Lambda = 53°$

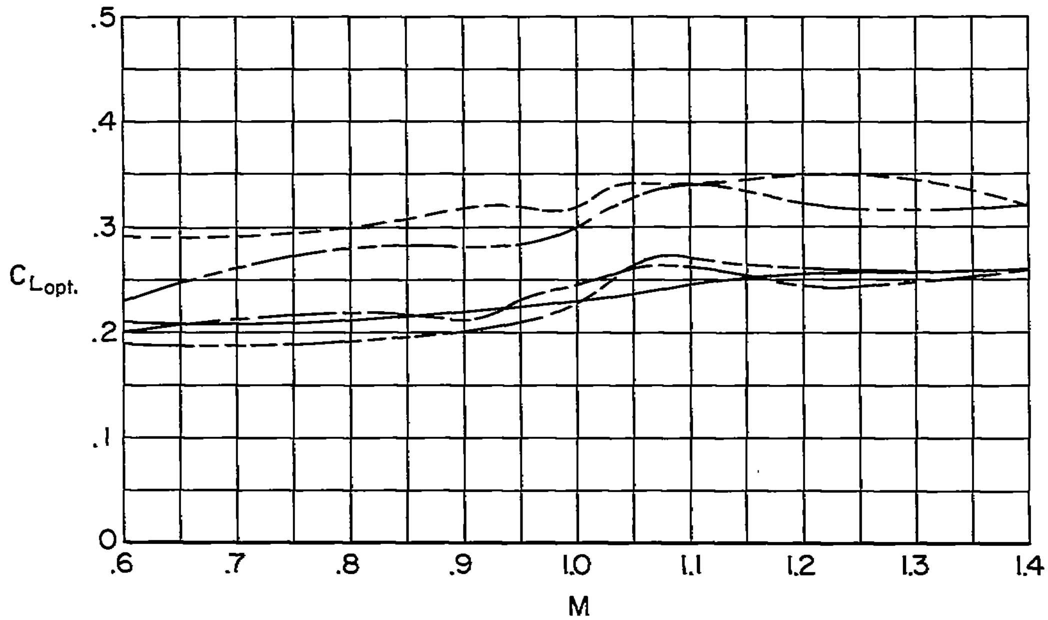

(b) $\Lambda = 63°$

Figure 9.- Variation of optimum lift coefficient with Mach number.

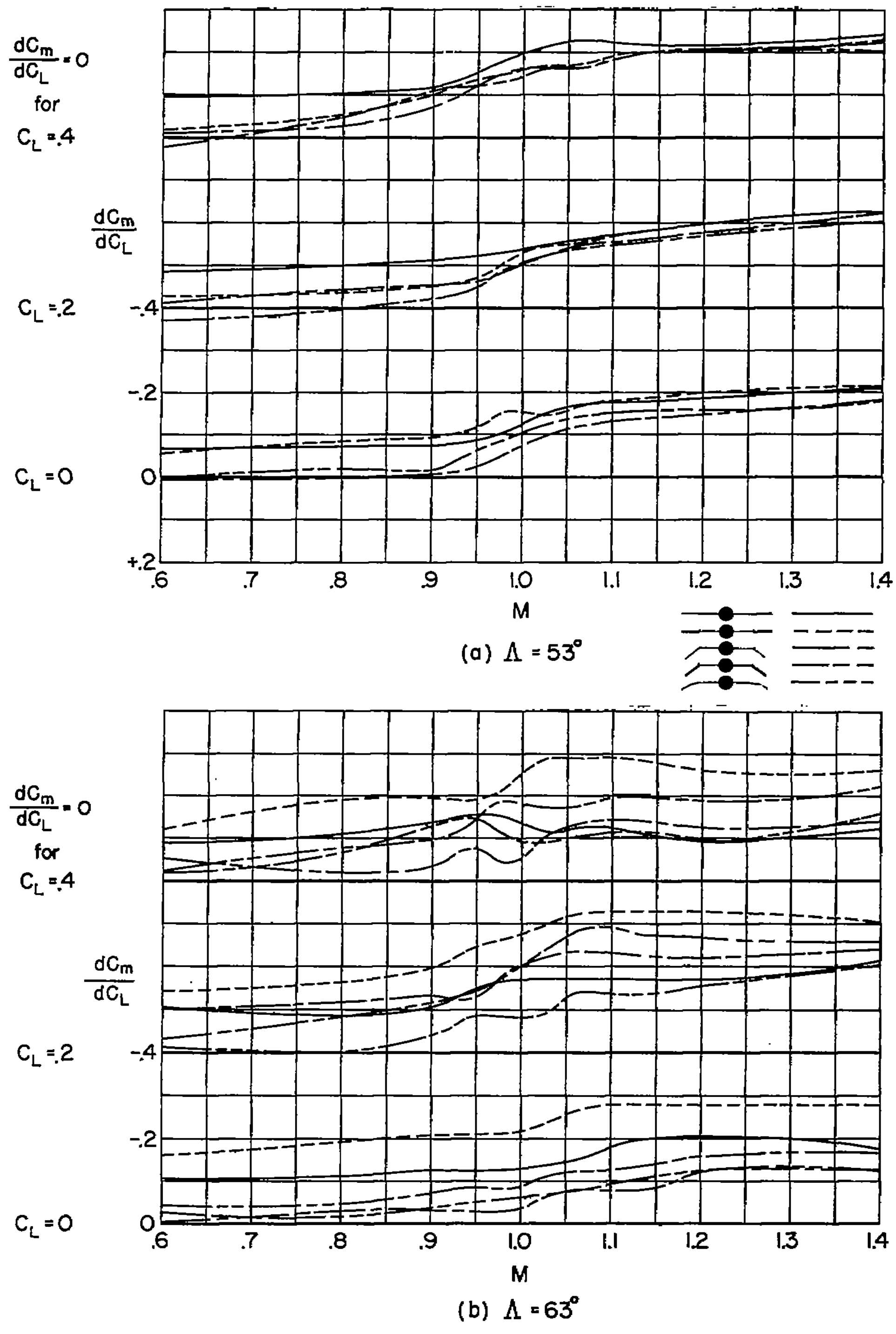

Figure 10.-Variation of pitching-moment-curve slope with Mach number at constant lift coefficient.

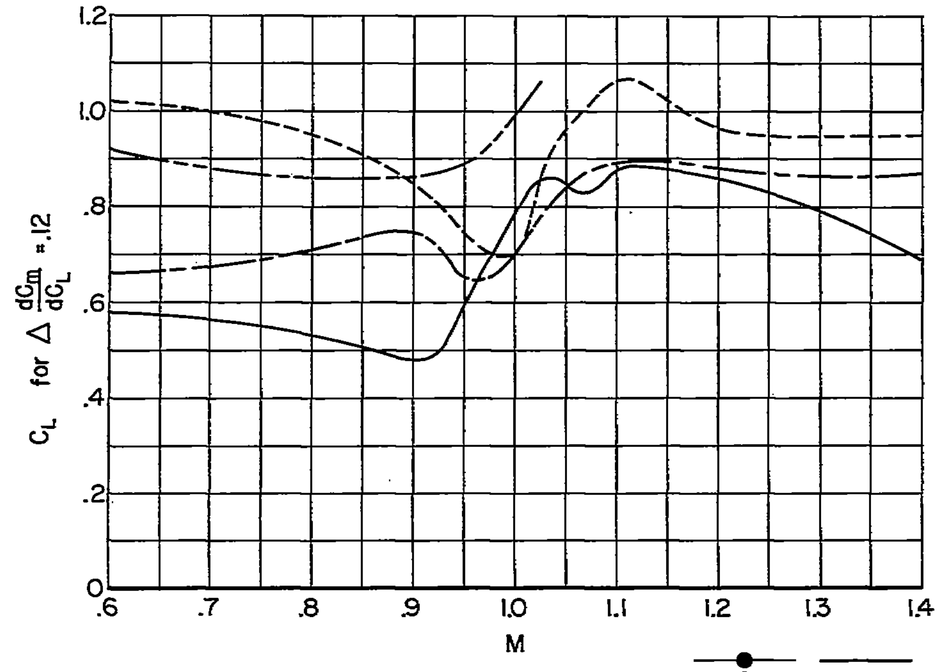

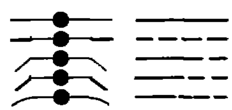

(a) $\Lambda = 53^\circ$

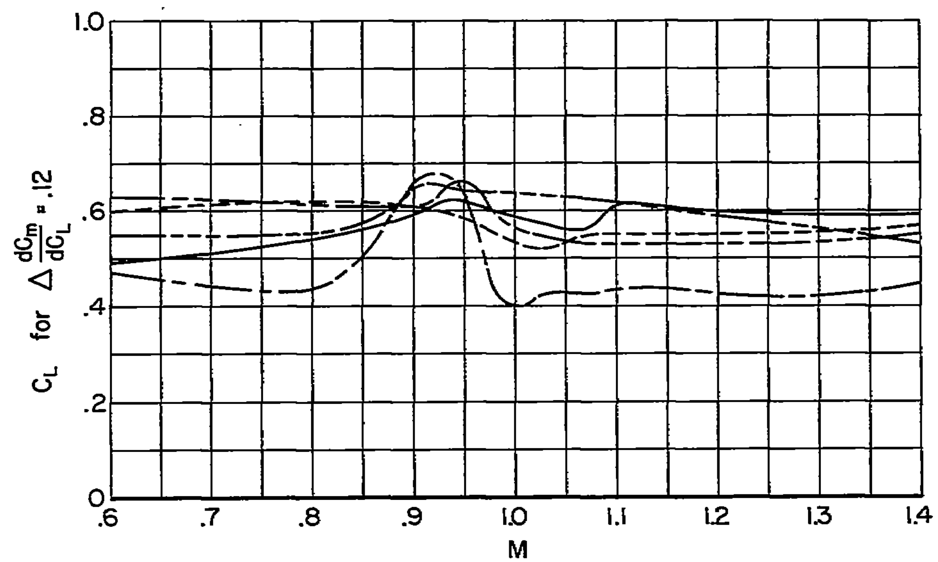

(b) $\Lambda = 63^\circ$

Figure 11.- Variation with Mach number of lift coefficient for $\Delta \frac{dC_m}{dC_L} = 0.12$.

NACA - Langley Field, Va.

 [redacted]

[redacted]